SUPPLEMENTARY INFORMATION

Immunity Depletion, Telomere Imbalance, and Cancer-associated Metabolism Pathway Aberrations in Intestinal Mucosa upon Short-Term Caloric Restriction

Evan Maestri, Kalina Duszka, Vladimir A Kuznetsov

Corresponding author:

Vladimir A Kuznetsov. E-mail: kuznetsv@upstate.edu

Supplementary Figure 1. Epithelial and immune system subcellular network

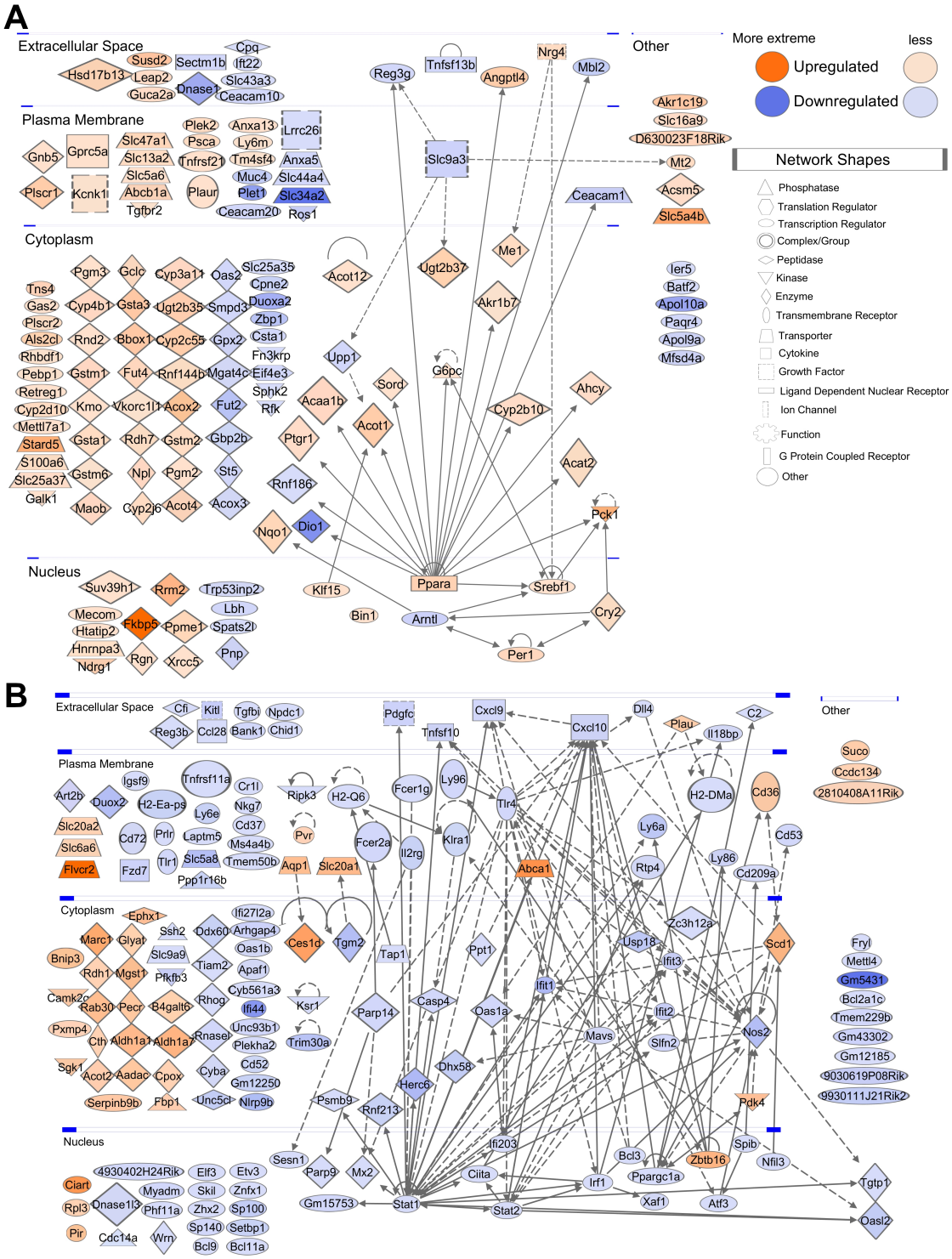

(A) Epithelial cells (EC) subcellular protein-protein interaction (PPI) network including 29 connected and 118 non-connected ECGs from DM distributed across four cellular compartments: extracellular space, plasma membrane, cytoplasm, nucleus. The ECG network contained 57 edges (protein interactions), average number of neighbors 2.28, clustering coefficient 0.06, network density 0.04, and protein-protein interaction (PPI) network enrichment $p < 1.00\ 10^{-16}$. The strongest hub for this network was Ppara (26 downstream, 4 upstream), which accounted for 26.3% (30/114) of the edges. **(B)** Immune system subcellular network including 68 connected and 103 non-connected ISGs. The ISG network contained 173 edges, average number of neighbors 3.72, clustering coefficient 0.18, network density 0.03, and PPI network enrichment $p < 1.00\ 10^{-16}$. The strongest hubs included Stat1 (36 downstream targets, 21 upstream targets), Tlr4 (19 downstream, 4 upstream), Stat2 (11 downstream, 5 upstream), Nos2 (10 downstream, 15 upstream), Ppargc1a (8 downstream, 6 upstream), and Cxcl10 (1 downstream, 16 upstream). Cellular locations of the gene hubs indicate Cxcl10 in the extracellular space, Tlr4 in the plasma membrane, Nos2 in the cytoplasm, and Stat1, Stat2, and Ppargc1a in the nucleus. In total, these proteins encoded by CR DEGs account for 43.9% (152/356) of the edges.

Supplementary Figure 2. Epithelial and immune system CR DEGs single-cell expression profiling

(A) Immune System CR DEGs

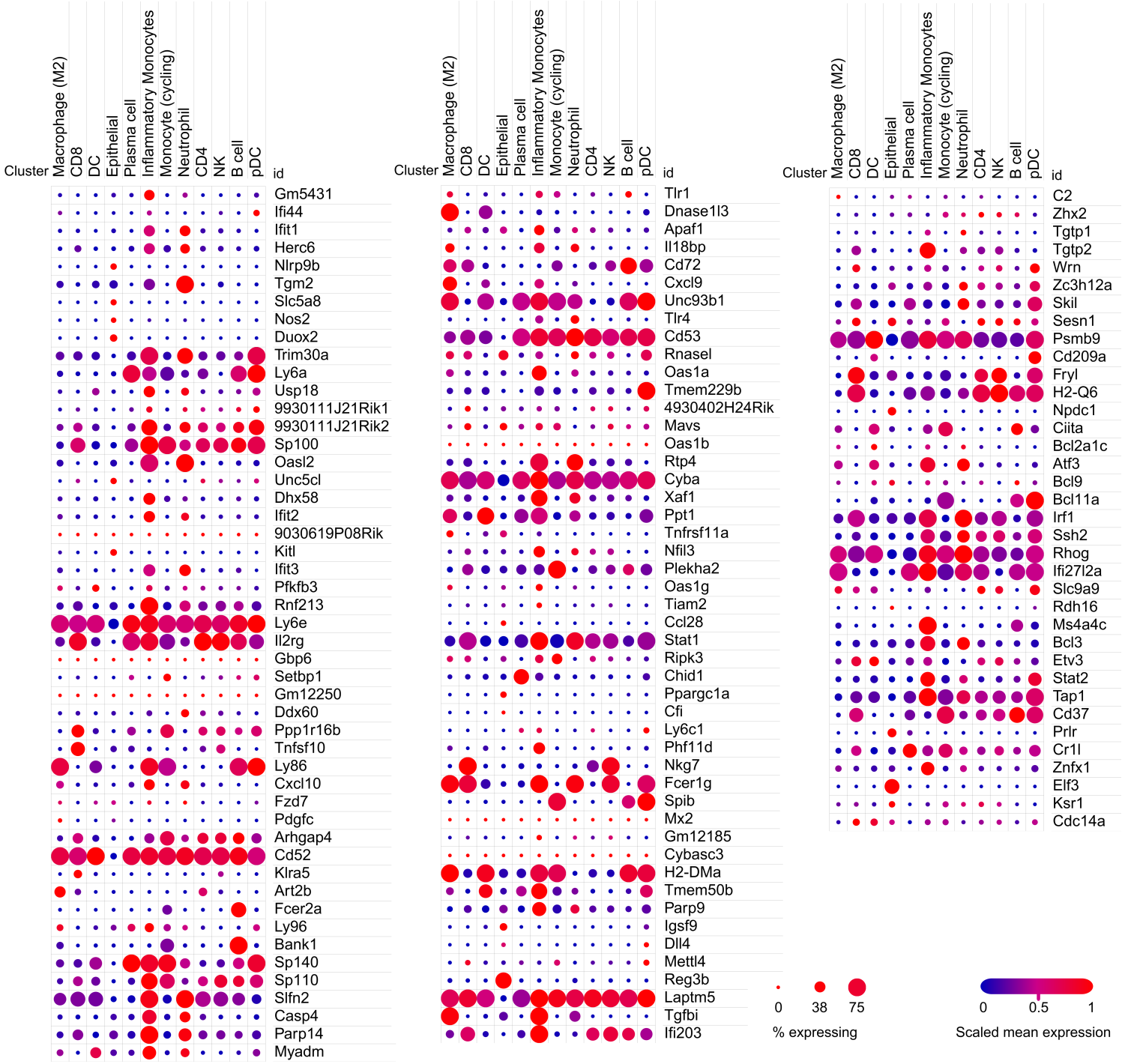

Single-cell RNA-seq expression in the murine small intestine visualized using the Broad Institute Single Cell Portal (SCP241, GSE106510). This plot includes 135 downregulated immune system genes. Genes located closer to the top and further left are more deeply suppressed (rows ordered by CR fold change). The plot shows the gene activity by expression magnitude (average expression) and prevalence (proportion of cells expressing the gene) across immune cell types. Dots are colored by scaled mean expression (which is relative to each gene's expression for all cells in each annotation column e.g., B cell). In the small intestine niche, the immune system is suppressed upon short-term CR.

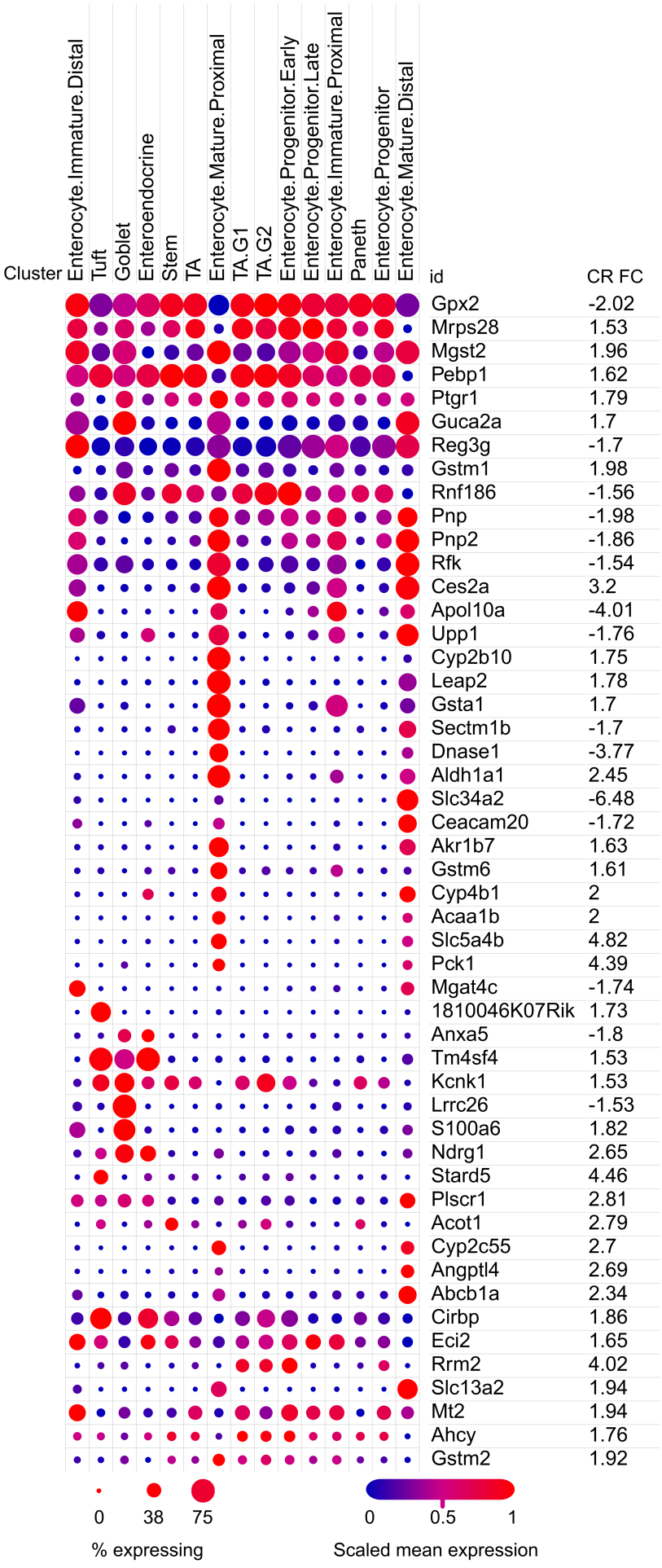

(B) Epithelial CR DEGs

Single-cell RNA-seq expression in the murine small intestine visualized using the Broad Institute Single Cell Portal (SCP44, GSE92332). This plot includes 50 highly differentially expressed CR DEGs with epithelial cell-type annotation specificity. The plot shows the gene activity by expression magnitude (average expression) and prevalence (proportion of cells expressing the gene) across epithelial cell types. This plot verifies our systems biology deconstruction of a mixture cell type tissue (epithelial/immune) giving enhanced cell-type specificity to epithelial annotated CR DEGs.

Supplementary Figure 3. NK, dendritic, phagocytic, and antigen presenting cell functional annotations network

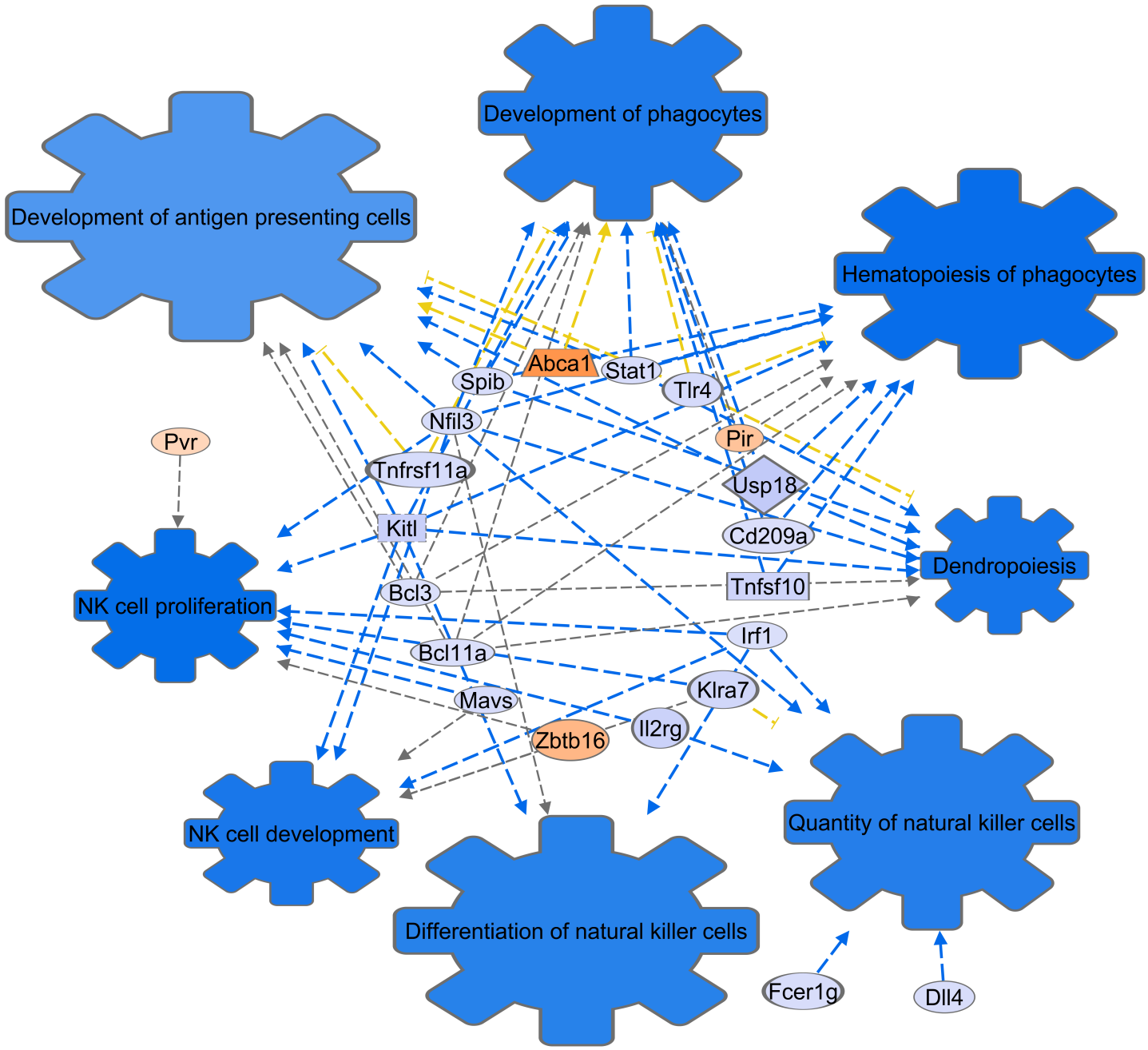

A network of 21 proteins encoded by CR DEGs based on the functional annotations of the 171 Immune System Genes. NK, dendritic, phagocytic, and antigen presenting cell associations within the Lymphoid Structure and Development IPA category were selected including development of phagocytes ($p = 1.29\ 10^{-08}$, $n = 13$), hematopoiesis of phagocytes ($p = 2.1\ 10^{-08}$, $n = 11$), development of antigen presenting cells ($p = 7.18\ 10^{-07}$, $n = 10$), dendropoiesis ($p = 2.19\ 10^{-06}$, $n = 8$), NK cell proliferation ($p = 7.31\ 10^{-06}$, $n = 8$), NK cell development ($p = 5.86\ 10^{-05}$, $n = 6$), quantity of natural killer cells ($p = 1.56\ 10^{-03}$, $n = 6$), and differentiation of natural killer cells ($p = 2.39\ 10^{-03}$, $n = 3$). Additional T lymphocyte annotations of the CR-induced immune DEGs included lack of T lymphocytes ($p = 2.93\ 10^{-6}$, $n = 5$), abnormal morphology of T lymphocytes ($p = 3.53\ 10^{-5}$, $n = 8$), abnormal morphology of Peyer's patches ($p = 8.54\ 10^{-4}$, $n = 4$), and lack of gamma-delta T lymphocytes ($p = 1.25\ 10^{-3}$, $n = 2$). Additional B lymphocyte annotations included: abnormal morphology of B lymphocytes ($p = 1.04\ 10^{-3}$, $n = 5$) and morphology of B-cell follicle ($p = 2.04\ 10^{-3}$, $n = 4$). These T and B cell annotations were not included in Figure 4 due to lack of IPA predicted z-score information for activation or inhibition.

Supplementary Figure 4. Immune system, epithelial, and cancer-associated subset network interactions

(A) The cancer-associated and immune PPI network contained 93 CR DEGs, 245 edges, average number of neighbors 3.63, clustering coefficient 0.16, network density 0.02, and PPI network enrichment $p < 1\ 10^{-16}$. **(B)** The cancer and epithelial network contained 68 DEGs, 186 edges, average number of neighbors 3.62, clustering coefficient 0.12, network density 0.03, and PPI network enrichment $p < 1\ 10^{-16}$. Non-connected proteins are not displayed. Blue indicates downregulated proteins and orange indicates upregulated proteins. Color intensity is based on the expression fold changes of the genes. Understanding the tumor-immune, immune-epithelial, and tumor-epithelial microenvironment interactions could explain CR malignancy risks and inform therapeutic strategies.

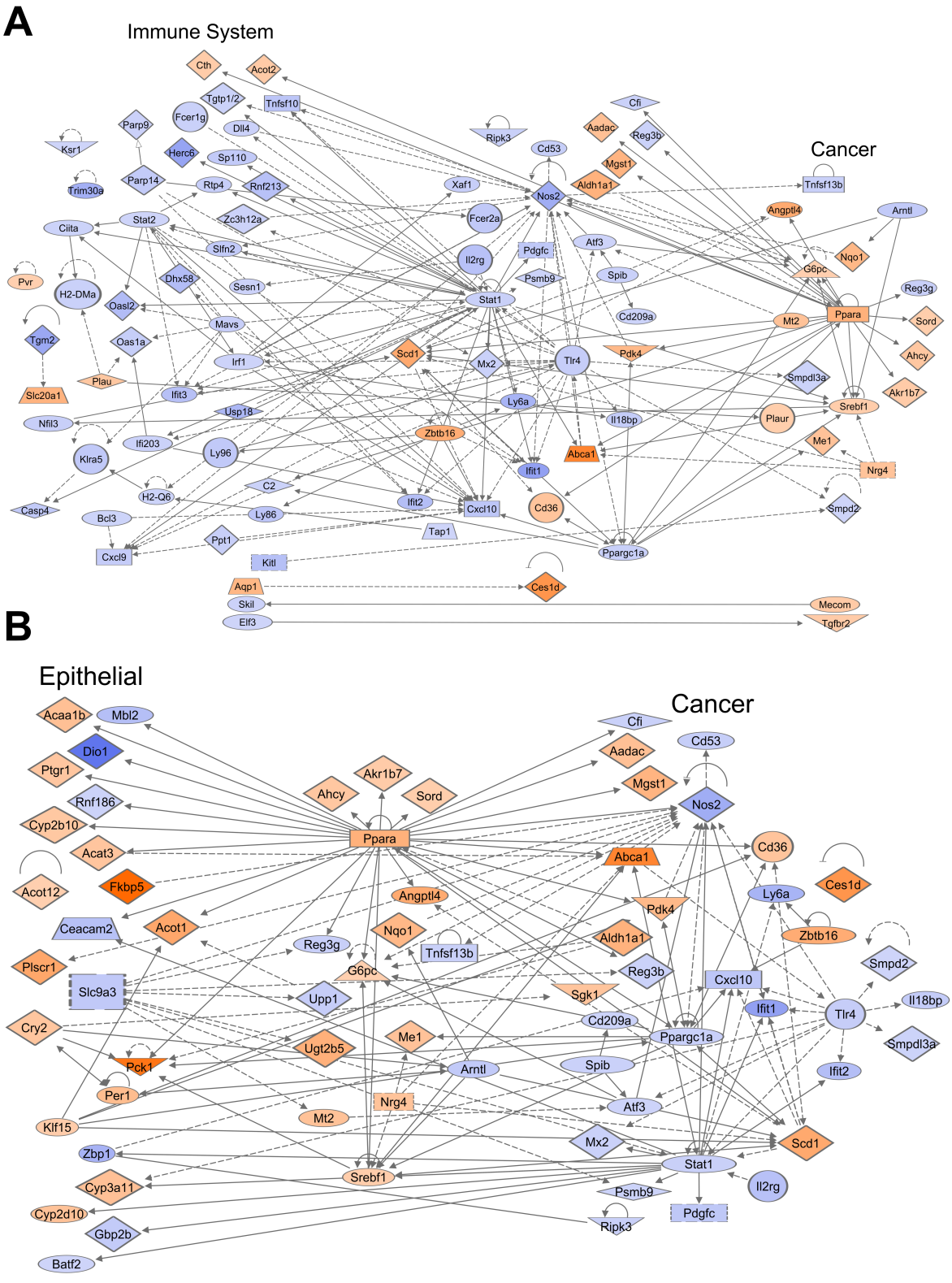

Supplementary Figure 5. Liver tissue 3-week CR comparative analysis

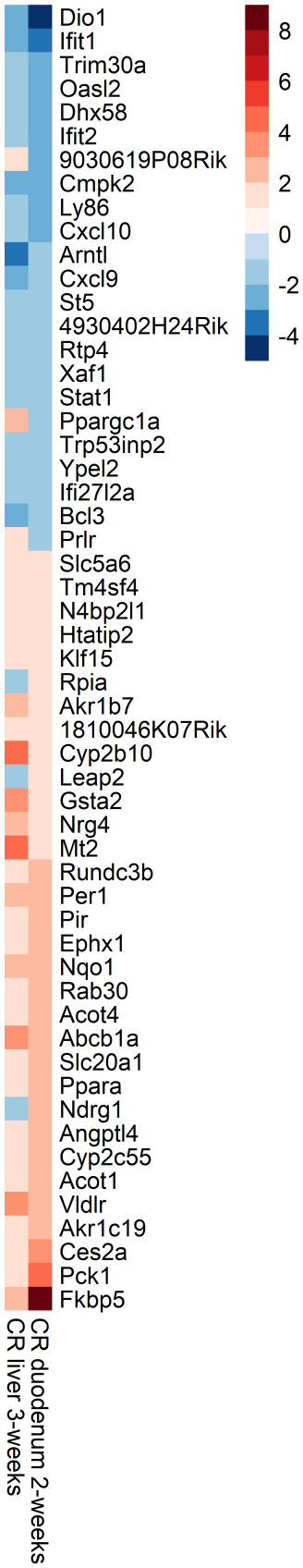

Comparison betweenthe DEG sets found in duodenum and liver short-term CR studies. The liver study used a 3-week CR at 75% of the diet as ad lib feeding (E-GEOD-51885, GSE51885). Our duodenal study used a 2-week CR at 75% of the diet as ad lib feeding. After selecting $p<0.05$, FC>1.1 from the liver DEGs, we compared the liver DEGs to our 505 CR duodenal DEGs. This revealed 55 genes commonly regulated in duodenum and liver upon short-term CR. In the liver and duodenum under CR conditions, 49/55 genes (89%) regulated had matched directionality fold changes.

Supplementary Figure 6. Interferon-inducible GTPase paralogs

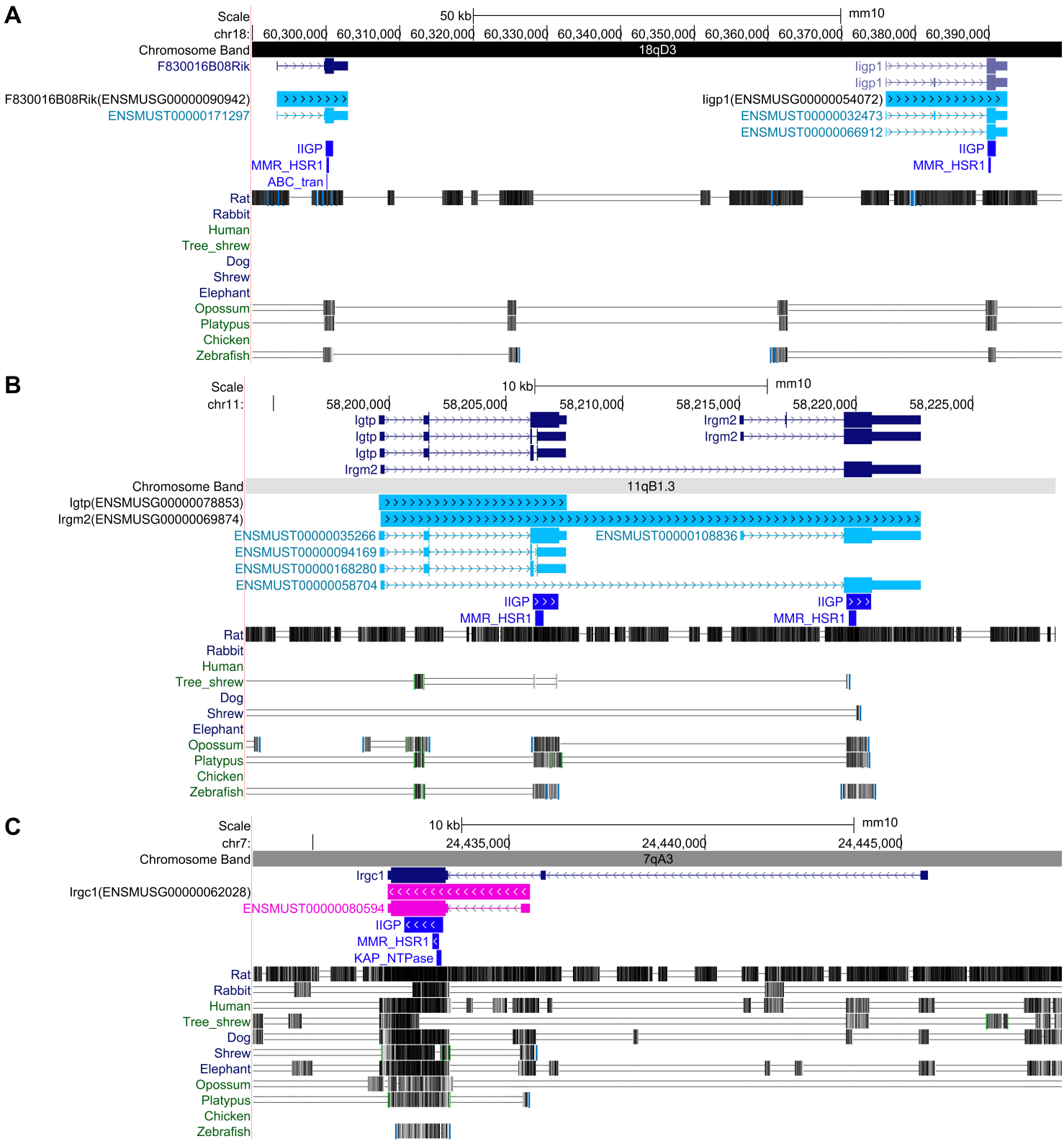

UCSC genome browser tracks defining four paralogs of the interferon-inducible GTPase family: **(A)** F830016B08Rik, Iigp1, **(B)** Irgm2, Igtp, **(C)** Irgc1. Annotation tracks are from Ensembl (Build 75) and RefSeq genome assembly (GRCm38.p5). Pfam-A domains are identified by software HMMER3: IIGP (Interferon-inducible GTPase; PF05049), MMR_HSR1(50S ribosome-binding GTPase; PF01926), ABC_tran (ABC transporter; PF00005), KAP_NTPase (KAP family P-loop domain; PF07693). The "Multiz alignments" track for mouse genome assembly (mm10) provided multiple alignment data combining PhyloP and PhastCons methods and shows the results of measurements of evolutionary conservation using these methods from the PHAST package for 60 vertebrates and three subsets (Glires, Euarchontoglires and placental mammal).

Supplementary Figure 7. A model of CR-induced mucosal cells and pathway responses in DM

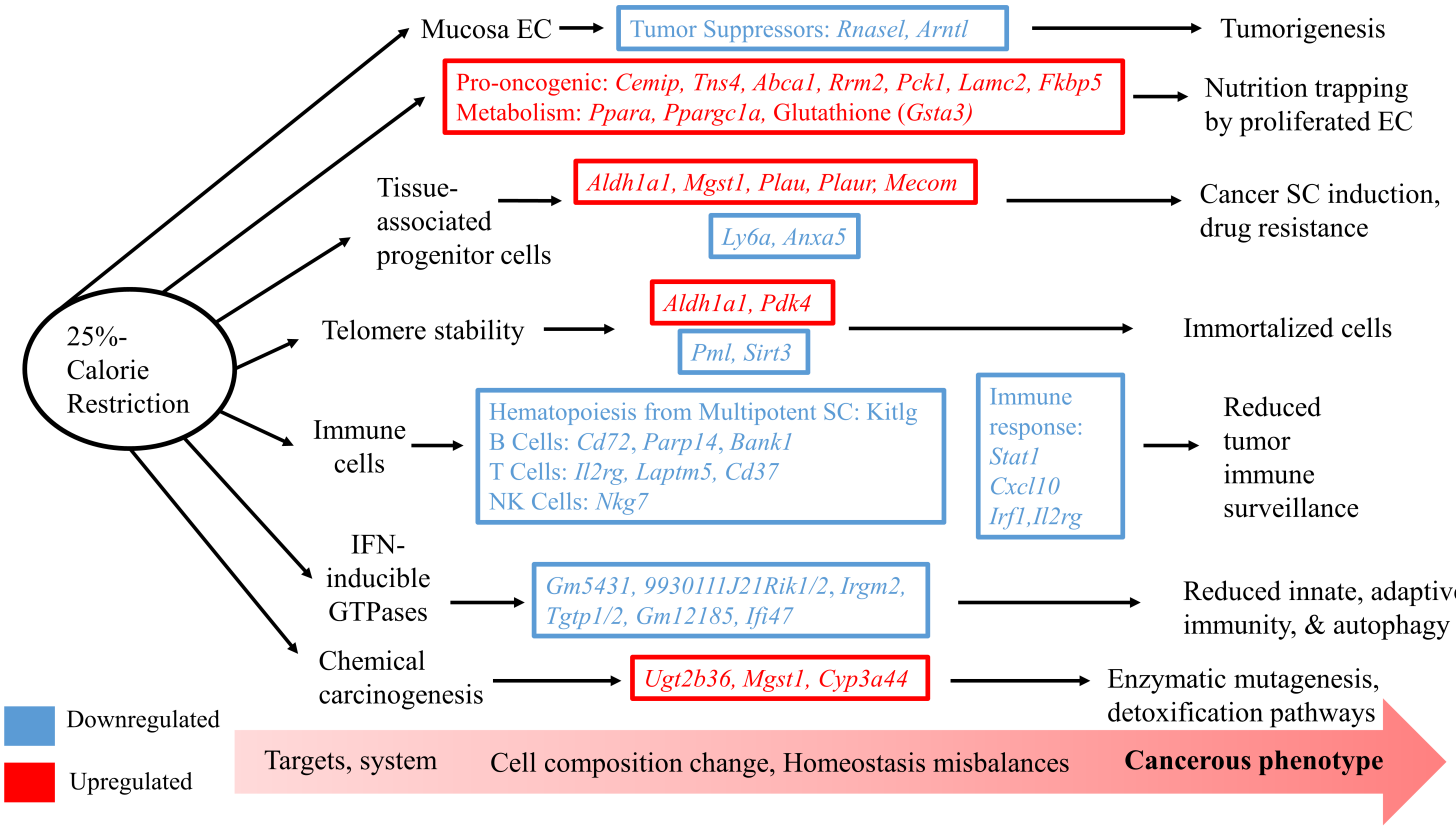

A model of CR-induced tumorigenesis in mucosa proposes activation of transcription of specific categories of genes involved in cell cycle, telomere stability regulation, stem-like tumor cells, chemical carcinogenesis including enzymatic mutagenesis genes, and cancer-related pathways mediated by metabolic reprogramming. However, it also depletes immune system and INF-inducible GTPases activity, leading to dysregulation of regulatory networks, cell types balances, activation of tumorigenesis pathways, cell-cell interactions, and drug resistance (see also Figure 10). Notice: Epithelial Cell (EC); Stem Cells (SC).

Supplementary Table 1. Functional enrichments common between human and mouse

(A) GO Biological Process

term ID	term description	human observed gene count	human background gene count	human FDR	mouse observed gene count	mouse background gene count	mouse FDR
GO:0009617	response to bacterium	34	555	9.41E-07	44	566	2.47E-13
GO:0002376	immune system process	111	2370	1.01E-15	78	1703	1.42E-12
GO:0006950	response to stress	112	3267	4.17E-08	103	2899	1.41E-10
GO:0051607	defense response to virus	27	181	1.30E-12	21	152	5.17E-10
GO:0051704	multi-organism process	80	2222	2.83E-06	74	1840	1.87E-09
GO:0044281	small molecule metabolic process	79	1779	6.76E-10	61	1489	8.80E-08
GO:0045087	innate immune response	44	676	1.32E-09	32	534	4.95E-07
GO:0032787	monocarboxylic acid metabolic process	32	477	3.86E-07	26	426	9.48E-06
GO:0071345	cellular response to cytokine stimulus	49	953	1.22E-07	33	676	2.12E-05
GO:0006082	organic acid metabolic process	47	959	9.47E-07	36	794	2.84E-05
GO:0005996	monosaccharide metabolic process	19	198	3.32E-06	14	148	8.03E-05
GO:0031667	response to nutrient levels	27	455	3.88E-05	25	461	9.48E-05

(B) GO Molecular Function

term ID	term description	human observed gene count	human background gene count	human FDR	mouse observed gene count	mouse background gene count	mouse FDR
GO:0043167	ion binding	154	6066	1.70E-03	141	5302	1.45E-06
GO:0052689	carboxylic ester hydrolase activity	10	139	1.41E-02	13	132	1.00E-04
GO:0015081	sodium ion transmembrane transporter activity	13	164	2.20E-03	13	138	1.50E-04
GO:0016788	hydrolase activity, acting on ester bonds	31	713	2.20E-03	30	660	1.70E-04
GO:0005102	signaling receptor binding	54	1513	9.60E-04	51	1515	2.80E-04
GO:0016290	palmitoyl-CoA hydrolase activity	4	10	4.30E-03	5	14	8.40E-04
GO:0004364	glutathione transferase activity	10	25	2.49E-07	6	28	1.20E-03
GO:0000166	nucleotide binding	63	2097	7.60E-03	58	2006	2.60E-03
GO:0008144	drug binding	53	1710	1.09E-02	48	1630	5.60E-03
GO:0016740	transferase activity	68	2250	4.30E-03	56	2110	1.76E-02
GO:0030246	carbohydrate binding	13	270	4.24E-02	13	265	1.91E-02

(C) KEGG Pathways

human term ID	mouse term ID	term description	human observed gene count	human background gene count	human FDR	mouse observed gene count	mouse background gene count	mouse FDR
hsa00983	mmu00983	Drug metabolism - other enzymes	17	76	3.08E-10	19	86	2.64E-12
hsa01100	mmu01100	Metabolic pathways	56	1250	1.71E-07	60	1296	5.33E-10
hsa05204	mmu05204	Chemical carcinogenesis	15	76	7.05E-09	15	92	2.53E-08
hsa00480	mmu00480	Glutathione metabolism	13	50	7.05E-09	11	61	1.20E-06
hsa00830	mmu00830	Retinol metabolism	7	62	3.80E-03	11	89	3.18E-05
hsa01040	mmu01040	Biosynthesis of unsaturated fatty acids	7	23	3.03E-05	7	27	3.78E-05
hsa03320	mmu03320	PPAR signaling pathway	10	72	7.57E-05	10	85	1.20E-04
hsa05200	mmu05200	Pathways in cancer	26	515	2.70E-04	25	522	1.50E-04
hsa01524	mmu01524	Platinum drug resistance	11	70	1.03E-05	9	76	2.70E-04

(D) Reactome Pathways

human term ID	mouse term ID	term description	human observed gene count	human background gene count	human FDR	mouse observed gene count	mouse background gene count	mouse FDR
HSA-1430728	MMU-1430728	Metabolism	99	2032	2.48E-15	79	1685	2.16E-13
HSA-211859	MMU-211859	Biological oxidations	28	214	5.36E-12	25	237	6.97E-10
HSA-168256	MMU-156590	Immune System	81	1925	2.87E-09	7	31	2.60E-04
HSA-156590	MMU-168256	Glutathione conjugation	11	33	5.80E-08	48	1523	1.90E-03
HSA-168249	MMU-168249	Innate Immune System	38	1012	4.30E-03	30	879	1.10E-02

Tables are ordered by individual mouse FDR (STRING v11, FDR <0.05).

Supplementary Table 2. (A) Upregulated cell cycle periodic genes (CycleBase)

Human Gene Symbol	Mouse Gene Symbol	Ensemble ID	Gene Description	FC	adj. P-value	Cell Cycle Phase	Literature (PubMed PMID)
FKBP5	Fkbp5	ENSMUSG00000024222	fk506 binding protein 5	8.54	9.35E-04	S	23936393, 21119664, 21498116
FKBP5 could be a biomarker for tumourigenesis (through the AKT singalling pathway) and chemoresistance. High FKBP51 levels decreased AKT phosphorylation and increased chemosensitivity, whereas low FKBP51 levels increased AKT phosphorylation and decreased chemosensitivity. Downregulation of FKBP5 desensitized pancreatic and breast cancer cell lines to several different classes of chemotherapeutic agents. FKBP5 genetic variation influences response to gemcitabine treatment of pancreatic cancer.							
RRM2	Rrm2	ENSMUSG00000020649	ribonucleotide reductase M2	4.02	2.05E-04	S	31363169, 20122995, 23113760, 20927319, 31417867, 17404105, 27551518
Ribonucleoside-diphosphate reductase subunit M2, Rrm2, in mouse (RRM2 in human) encodes one of the small subunits of ribonucleotide reductase (RR), the rate limiting enzyme for production of deoxyribonucleotides. In both mouse and human cells this gene provides regulation of cell cycle processes and is activated by E2F1 and EZH2 DNA binding in gene promoter regions. RRM2 associates with RRM1 forming an active RR. Its accumulation plays a central role in providing precursors necessary for DNA synthesis catalyzing the biosynthesis of deoxyribonucleotides. RRM2 plays active roles in tumorigenesis and is a poor prognostic factor for cancers, such as colon, breast and pancreatic. It is involved in colorectal cancer metabolic reprogramming and siRNA knockdown of RRM2 in vitro and in vivo reduced cell proliferation.							
ACSL3	Acsl3	ENSMUSG00000032883	acyl-CoA synthetase long-chain family member 3	2.11	6.33E-03	G1	30008815
ACSL3 is associated with disease and especially with several cancers, can promote cancer cell survival through amplified fatty acid β-oxidation and increased arachidonic acid-dependent prostaglandin synthesis, both of which can drive tumor growth.							
GAS2L3	Gas2l3	ENSMUSG00000074802	growth arrest-specific 2 like 3	1.81	2.16E-02	G2	22344256, 23469016, 24571573, 19139817
Cytotoxic immunoconjugates which target and eliminate gastric cancer cells showed consistent downregulation responses of GAS2L3 in whole genome microarray expression profiling (validated using RTQ-PCR). GAS2L3 is necessary for proper cytokinesis and for abscission, the final step of cytokinesis that results in separation of the daughter cells. GAS2L3 is specifically expressed in mitosis and localizes to the spindle midzone/midbody and the constriction zone during cytokinesis. It mediates interactions with components of the so-called chromosome passenger complex consisting of the mitotic kinase Aurora B and associated proteins.							
OPN3	Opn3	ENSMUSG00000026525	opsin 3	1.74	9.67E-03	G1	31802643, 29863164
OPN3 acted as an oncogene through enhancing metastasis in lung adenocarcinoma via its overexpression promoting epithelial-mesenchymal transition. Blue light-emitting diodes (LED) irradiation and reductive effect on colon cancer cell viability was reversed by Opn3 siRNA knockdown.							
RBBP8	Rbbp8	ENSMUSG00000041238	retinoblastoma binding protein 8	1.70	2.25E-02	S	31636387, 16249056
RBBP8 facilitates the G1/S transition promoting Cyclin D1 and CDK4 levels and G2/M cycle checkpoints in double-stranded break repair processes. RBB8 is overexpressed in both gastric cancer and high-grade intraepithelial neoplasia tissues (HGIEN). Knockdown of RBBP8 inhibited cell proliferation and colony formation in gastric cancer. CtIP (also known as RBBP8) interacts with tumor suppressors, such as BRCA1. Ctip(-/-) embryo cells are arrested in G1 and do not enter S phase.							
PUS7	Pus7	ENSMUSG00000057541	pseudouridylate synthase 7 homolog (S. cerevisiae)	1.64	2.43E-02	G1	31451225, 31433208, 30008265
PUS7 may be a potential biomarker of glioma. It is involved in transcriptome reprogramming by cancer exosomes, which could lead to cancer-associated pathologies, immune evasion/modulation, and cell fate alteration/metastasis. PUS7 is an interactor of SIRT1, involved in the sirtuin signaling pathway.							
ABCC5	Abcc5	ENSMUSG00000022822	ATP-binding cassette, sub-family C (CFTR/MRP), member 5	1.62	6.93E-03	S	15897250, 25640272
Multidrug resistance proteins (MRPs) of the ABCC subfamily (including ABCC5) are involved in increased cellular efflux and resistance to fluoropyrimidine-based therapy. ABCC5 confers resistance to 5'-Fluorouracil (5-FU), used in the treatment of colon and breast cancers. Membrane transporters prevent anticancer drugs from reaching target intracellular concentrations. ABCC5 is an efflux transporter for cyclic nucleotides and nucleic acid analogs. Endogenous ABCC5 siRNA-mediated silencing increased 5-FU cellular cytotoxicity and enhanced accumulation of its metabolites.							
KMO	Kmo	ENSMUSG00000039783	kynurenine 3-monooxygenase (kynurenine 3-hydroxylase)	1.51	4.32E-02	G1	32339939, 26099564
Kynurenine 3-monooxygenase (KMO) is a pivotal enzyme of the kynerenine pathway (KP) involved in tryptophan (Trp) metabolism, which generates several toxic metabolites responsible for inflammatory disorders. KP enzymes are involved in cancer progression and may be a key biomarker for liver cancer. KMO positively regulated proliferation, migration, and invasion of human hepatocellular carcinoma (HCC). Kynurenin from cancer cells binds to the aryl hydrocarbon receptor (AHR) on T cells and suppresses T cell proliferation and oncolytic activities, attenuating anticancer immunity.							

Supplementary Table 2. (B) Downregulated cell cycle periodic genes (CycleBase)

Human Gene Symbol	Mouse Gene Symbol	Ensemble ID	Gene Description	FC	adj. P-value	Cell Cycle Phase	Literature (PubMed PMID)
IFIT1	Ifit1	ENSMUSG00000034459	interferon-induced protein with tetratricopeptide repeats 1	-3.36	2.57E-03	G1	31372503
Functions in antiviral response. Ifit1 knockout promoted viral replication in murine norovirus infected cells.							
TGM2	Tgm2	ENSMUSG00000037820	transglutaminase 2, C polypeptide	-3.10	4.48E-03	G1	31010374, 28754668, 31570702
TGM2 is an apoptosis attenuator and related to cancer stem cell survival/tumor formation in multiple cancers. Its inhibition reversed mesenchymal transdifferentiation in glioma stem cells. TGM2 levels are upregulated in CRC and CRC patients with high levels of TGM2 had lower survival. TGM2-siRNA interference inhibited wnt3a/β-catenin/cyclin D1 pathway in colorectal cancer cells, attenuating tumor growth in nude mice. TGM2 is transcriptionally activated by ETS1, inhibits apoptosis, and is associated with chemotherapy stress in CRC via activation of Wnt/β-catenin signaling.							
UNC5CL	Unc5cl	ENSMUSG00000043592	unc-5 homolog C (C. elegans)-like	-2.36	2.27E-04	G2	22158417, 30071397
Unc5CL is a factor in epithelial inflammation and immunity. It a candidate gene involved in mucosal diseases, such as inflammatory bowel disease. Many chemokines (IL-8, CXCL1 and CCL20) are downstream targets of Unc5CL. These pro-inflammatory markers orchestrate the initial recruitment of immune cells and Unc5CL could be involved in epithelial danger responses. Unc5CL is a member of the family of death domain (DD)-containing proteins involved in many cellular processes, including apoptosis, inflammation, and development. Unc5CL is an inducer of proinflammatory signaling cascades leading to activation of NF-κB and JNK. It also has high specific tissue distribution in mucosal epithelia (including the intestine), and the protein is sorted to the apical face of these cells.							
IFIT2	Ifit2	ENSMUSG00000045932	interferon-induced protein with tetratricopeptide repeats 2	-2.30	6.83E-03	G1	29316541
IFIT2 knockdown significantly increased proliferation, migration, and invasion of human gastric cancer cell lines.							
PAQR4	Paqr4	ENSMUSG00000023909	progestin and adipoQ receptor family member IV	-1.76	4.09E-04	S	29228296, 30322804, 28992327
PAQR4 (Progestin and AdipoQ Receptor 4) expression is closely associated with progression of many cancers and microRNA (miRNA) processing. miR-370 inhibited cell proliferation, invasion and epithelial-to-mesenchymal transition (EMT) of gastric cancer (GC) cells by directly down-regulating PAQR4 expression. Knockdown of PAQR4 supressed cell proliferation in human breast cancer cells. PAQR4 is highly expressed in human breast cancers. The steady state of CDK4 (crucial for G1-to-S transition) is controlled by PAQR4. PAQR4 knockdown reduces cell proliferation accompanied by decreased CDK4 levels. PAQR4-deleted mice are resistant to chemical carcinogen-induced tumor formation.							
STAT1	Stat1	ENSMUSG00000026104	signal transducer and activator of transcription 1	-1.66	2.37E-03	G2	22190859, 11323675, 12093877, 15891579, 30235866
STAT1 can suppress tumor formation. The elimination of interferon (IFN)-γ, or STAT1 genes (thus lacking interferon-mediated pathways) in mice resulted in increased incidence and growth of spontaneous and chemically-induced tumors. Deficiency in STAT1 signaling predisposes gut inflammation and prompts colorectal cancer development							
CDKL5	Cdkl5	ENSMUSG00000031292	cyclin-dependent kinase-like 5	-1.66	1.57E-02	S	31858726, 17589290, 28740074
Cyclin-dependent kinase-like 5 (CDKL5) is highly expressed in gliomas, and CDKL5 overexpression promotes invasion, proliferation, migration and drug resistance of glioma cells. CDKL5 acts through the phosphoinositide 3-kinase (PI3K)/AKT axis. CDKL5 is also a potential target for immuotherapy in adult T-cell leukemia. CDKL5 localizes at the centrosome and at the midbody in proliferating cells and is required for faithful cell division. Acute inactivation of CDKL5 by RNA interference (RNAi) leads to multipolar spindle formation, cytokinesis failure and centrosome accumulation.							
IER5	Ier5	ENSMUSG00000056708	immediate early response 5	-1.54	1.28E-03	S	28430589, 29104487, 26754925
The immediate early response gene 5 (IER5) is a radiation response gene involved in DNA damage and repair. IER5 induced by radiation dose enhanced apoptosis of cervical cancer, was inversely associated with tumor size. IER5 is upregulated in several cancers and contributes to proliferation of cells under stressed conditions.							

Supplementary Table 3. The 171 Immune system genes characterized using the Disease and Biological Function annotation tool from IPA

(A)

Category	p-value	Molecules
Endocrine System Disorders	1.1E-38-2.66E-04	59
Gastrointestinal Disease	1.1E-38-2.9E-03	80
Immunological Disease	1.1E-38-2.48E-03	73
Metabolic Disease	1.1E-38-2.7E-03	60
Cellular Growth and Proliferation	4.07E-19-2.39E-03	64
Lymphoid Tissue Structure and Development	4.07E-19-2.94E-03	66
Infectious Diseases	1.26E-17-2.94E-03	37
Cell-To-Cell Signaling and Interaction	2.47E-16-2.57E-03	47
Immune Cell Trafficking	2.47E-16-2.94E-03	51
Inflammatory Response	2.47E-16-2.94E-03	77
Antimicrobial Response	1.62E-14-6.6E-04	21
Tissue Morphology	7.65E-13-2.92E-03	58
Cellular Function and Maintenance	1.87E-12-2.39E-03	55
Cell Death and Survival	8.81E-12-2.94E-03	68
Connective Tissue Disorders	1.19E-09-1.23E-03	24
Inflammatory Disease	1.19E-09-2.3E-03	46

(A) Disease and Biological category annotations for the 171 Immune system gene subset. P-values indicate category dynamical range (all $p<0.01$), calculated by Fisher's Exact Test. **(B)** Disease annotations for the IPA Lymphoid Tissue Structure and Development category. **(C)** Disease annotations for the IPA Inflammatory Response category.

(B)

Diseases or Functions Annotation	p-value	Activation z-score	# Molecules
B cell annotations			
Proliferation of B lymphocytes	9.52E-10	-1.033	18
Quantity of B lymphocytes	3.58E-06	-0.257	17
Proliferation of pre-B lymphocytes	4.99E-04	-0.837	4
Abnormal morphology of B lymphocytes	1.04E-03		5
Proliferation of pro-B lymphocytes	1.73E-03		3
Differentiation of B lymphocytes	1.90E-03		8
Morphology of B-cell follicle	2.04E-03		4
T cell annotations			
Cell proliferation of T lymphocytes	1.20E-09	0.88	25
T cell development	5.12E-09	-1.255	24
Quantity of T lymphocytes	3.66E-07	-0.084	23
Lack of T lymphocytes	2.93E-06		5
Differentiation of T lymphocytes	3.94E-06	-1.545	16
Quantity of CD8+ T lymphocyte	1.53E-05	-1.156	10
Abnormal morphology of T lymphocytes	3.53E-05		8
Quantity of helper T lymphocytes	1.99E-04	1.379	7
Quantity of CD4+ T-lymphocytes	2.14E-04	-0.042	9
Quantity of intraepithelial T lymphocytes	3.99E-04		3
Differentiation of Th2 cells	6.16E-04	1.4	5
Quantity of double-negative T lymphocyte	6.96E-04	-1.387	5
Abnormal morphology of Peyer's patches	8.54E-04		4
Lack of gamma-delta T lymphocytes	1.25E-03		2
Quantity of natural killer T lymphocytes	2.92E-03		4
NK, phagocytic, dendritic, and antigen presenting cell annotations			
Development of phagocytes	1.29E-08	-1.576	13
Hematopoiesis of phagocytes	2.10E-08	-2.208	11
Development of antigen presenting cells	7.18E-07	-1.035	10
Dendropoiesis	2.19E-06	-1.756	8
NK cell proliferation	7.31E-06	-2.393	8
NK cell development	5.86E-05		6
Quantity of natural killer cells	1.56E-03	-1.467	6
Differentiation of natural killer cells	2.39E-03		3

(C)

Diseases or Functions Annotation	p-value	Activation z-score	# Molecules
Activation of leukocytes	2.5E-16	-0.544	32
Antimicrobial response	1.6E-14		20
Antiviral response	5.3E-14		16
Inflammation of absolute anatomical region	1.3E-11	1.594	37
Inflammatory response	3.7E-09	-1.326	26
Activation of macrophages	8.4E-08	-0.336	12
Activation of phagocytes	1.1E-07	-0.342	14

B Cell genes:

Bank1,Bcl11a,Bcl3,Ccl28,Cd209a, Cd36,Cd72,Dll4,Fcer1g,Fcer2a,Il2rg , Kitl,Ly86,Ly96,Mavs,Nfil3,Nos2, Parp14,Plekha2,Rhog,Ripk3,Spib, Stat1,Tgfbi,Tlr4,Tnfrsf11a,Unc93b1,Z c3h12a

T Cell genes:

Apaf1,Art2b,Bcl11a,Bcl3,Camk2g, Ccdc134,Cd209a,Cd37,Ciita,Cr1l, Cth,Cxcl10,Dll4,Elf3,Fcer1g,Fzd7, H2-DMa,H2-Q6,Il2rg,Irf1,Kitl,Klra7, Ksr1, Laptm5, Ly6a,Mavs,Nfil3, Nos2,Plau,Psmb9,Pvr,Ripk3,Skil, Slc6a6,Spib, Stat1,Stat2,Tap1,Tlr4, Tnfrsf11a,Tnfsf10,Trim30a,Usp18, Zbtb16,Zc3h12a

NK genes:

Dll4,Fcer1g,Il2rg,Irf1,Kitl,Klra7, Mavs, Nfil3,Pvr,Zbtb16

Inflammatory response genes:

Atf3,Ccl28,Cd209a,Cd36,Cd37,Ciita, Cr1l,Cxcl10,Cxcl9,Fcer1g,Kitl,Mavs, Nos2,Pdk4,Pfkfb3,Plau,Ppt1,Reg3a, Ripk3,Rnasel,Stat1,Tgm2,Tlr4, Tnfrsf11a,Usp18,Zbtb16

Supplementary Table 4. CR-responded cancer stem cell related genes

(A)

Ensemble ID	Gene Symbol	Gene Description	FC	adj. P-value
ENSMUSG00000020826	*Nos2*	nitric oxide synthase 2, inducible	-2.92	1.39E-02
ENSMUSG00000075602	*Ly6a*	lymphocyte antigen 6 complex, locus A	-2.67	1.05E-03
ENSMUSG00000019966	*Kitl*	kit ligand	-2.25	8.00E-03
ENSMUSG00000031304	*Il2rg*	interleukin 2 receptor, gamma chain	-2.18	1.62E-04
ENSMUSG00000028019	*Pdgfc*	platelet-derived growth factor, C polypeptide	-1.96	3.73E-03
ENSMUSG00000027712	*Anxa5*	annexin A5	-1.80	3.84E-02
ENSMUSG00000039005	*Tlr4*	toll-like receptor 4	-1.77	1.23E-03
ENSMUSG00000027314	*Dll4*	delta-like 4 (Drosophila)	-1.61	1.31E-02
ENSMUSG00000024371	*C2*	complement component 2 (within H-2S)	-1.59	1.99E-02
ENSMUSG00000071757	*Zhx2*	zinc fingers and homeoboxes 2	-1.59	1.56E-03

(B)

Ensemble ID	Gene Symbol	Gene Description	FC	adj. P-value
ENSMUSG00000046223	*Plaur*	plasminogen activator, urokinase receptor	1.55	2.57E-02
ENSMUSG00000027684	*Mecom*	MDS1 and EVI1 complex locus	1.67	2.99E-02
ENSMUSG00000021822	*Plau*	plasminogen activator, urokinase	1.78	1.48E-03
ENSMUSG00000078566	*Bnip3*	BCL2/adenovirus E1B interacting protein 3	2.20	8.95E-03
ENSMUSG00000040584	*Abcb1a*	ATP-binding cassette, sub-family B (MDR/TAP), member 1A	2.34	2.27E-04
ENSMUSG00000008540	*Mgst1*	microsomal glutathione S-transferase 1	2.37	3.45E-04
ENSMUSG00000053279	*Aldh1a1*	aldehyde dehydrogenase family 1, subfamily A1	2.45	1.76E-04
ENSMUSG00000005125	*Ndrg1*	N-myc downstream regulated gene 1	2.65	1.48E-03

(A) Downregulated cancer stem cell related genes differentially regulated upon CR. **(B)** Upregulated cancer stem cell related genes differentially regulated upon CR. *Aldh1a1* was identified as both a cancer stem cell related gene and marker.

Supplementary Table 5. The 121 cancer-associated genes characterized using the Disease and Biological annotation tool from IPA

(A)

Category	p-value	Molecules
Metabolic Disease	4.17E-13-1.21E-03	38
Cancer	7.03E-12-2.64E-03	48
Humoral Immune Response	4.79E-11-2.98E-03	24
Gastrointestinal Disease	1.63E-10-2.86E-03	55
Endocrine System Disorders	2.1E-10-1.21E-03	32
Digestive System Development and Function	4.47E-10-1.6E-03	28
Immunological Disease	5.39E-10-2.86E-03	33
Lipid Metabolism	1.47E-09-2.73E-03	33
Small Molecule Biochemistry	1.47E-09-2.73E-03	37
Lymphoid Tissue Structure and Development	9.41E-09-2.49E-03	34
Immune Cell Trafficking	1.08E-08-2.64E-03	32
Carbohydrate Metabolism	1.25E-08-1.18E-03	24
Inflammatory Response	4.82E-08-2.64E-03	53
Cellular Function and Maintenance	2.75E-07-2.29E-03	40
Infectious Diseases	5.68E-07-1.18E-03	16

Metabolic Disease:

Abca1,Akr1b7,Angptl4,Arntl,Atf3,Cd209a,Cd36, Cxcl10,Ddx60,Fcer2a,G6pc,Gsta1,Ifit1,Ifit2, Igsf9,Il18bp,Ly6a,Maob,Me1,Mgst1,Nos2,Nqo1, Nrg4,Pdgfc,Ppara,Ppargc1a,Psmb9,Scd1,Spib, Srebf1,Stat1,Tap1,Tgfbr2,Tlr4,Tnfrsf21, Tnfsf13b,Upp1,Xaf1

Cancer:

Abca1,Angptl4,Atf3,Cd36,Cyba,Cyp2c55,Fut4, Galk1,Guca2a,Htatip2,Ifit1,Il18bp,Il2rg,Lamc2, Ly6a,Mecom,Mt2,Muc4,Ndrg1,Nos2,Nqo1, Nuak2,Pdgfc,Pdk4,Plaur,Ppara,Ppargc1a,Psmb9 ,Reg3a,Ripk3,Rpl3,Rrm2,Scd1,Setbp1,Slc6a6, Smpd3,Spib,Srebf1,Stat1,Tap1,Tff1,Tgfbr2,Tlr4,T nfrsf21, Tnfsf13b,Xaf1,Xrcc5,Zbtb16

(B)

Diseases or Functions Annotation	p-value	Activation z-score	Molecules	# Molecules
Abdominal neoplasm	7.03E-12	-0.594	Atf3,Cyp2c55,Fut4,Guca2a,Htatip2,Ly6a,Mt2,Muc4,Ndrg1,Nos2, Nuak2,Pdgfc,Ppara,Psmb9,Ripk3,Rrm2,Scd1,Tap1,Tff1,Tgfbr2,Tlr4, Xaf1,Xrcc5	23
Digestive organ tumor	1.63E-10	-0.943	Cyp2c55,Guca2a,Htatip2,Ly6a,Mt2,Muc4,Ndrg1,Nos2,Nuak2,Pdgfc, Ppara,Psmb9,Ripk3,Rrm2,Scd1,Stat1,Tap1,Tff1,Tgfbr2,Tlr4	21
Abdominal cancer	3.00E-10	-0.184	Atf3,Cyp2c55,Fut4,Htatip2,Ly6a,Mt2,Muc4,Ndrg1,Nos2,Pdgfc,Ppara, Psmb9,Ripk3,Rrm2,Scd1,Tgfbr2,Xaf1	17
Liver cancer	7.57E-08	-0.512	Cyp2c55,Htatip2,Mt2,Ndrg1,Nos2,Pdgfc,Ppara,Psmb9,Rrm2,Scd1, Tgfbr2	11
Abdominal carcinoma	7.96E-08	0.152	Tgfbr2,Scd1,Rrm2,Ripk3,Psmb9,Ppara,Pdgfc,Nos2,Mt2,Ly6a,Htatip2, Cyp2c55	12
Epithelial neoplasm	2.40E-07	0.585	Angptl4,Atf3,Cyp2c55,Htatip2,Ifit1,Ly6a,Mt2,Nos2,Nqo1,Nuak2, Pdgfc,Ppara,Psmb9,Reg3a,Ripk3,Rrm2,Scd1,Stat1,Tff1,Tgfbr2	20
Tumorigenesis of epithelial neoplasm	1.08E-04	0.317	Htatip2,Ifit1,Ly6a,Mt2,Nqo1,Nuak2,Pdgfc,Ppara,Psmb9,Rrm2,Stat1, Tff1,Tgfbr2	13

(A) Disease and Biological category annotations for the 121 cancer-associated gene subset. P-values indicate category dynamical range (all $p<0.01$), calculated by Fisher's Exact Test. **(B)** Disease annotations for the IPA Cancer category.

Supplementary Table 6. Selected up-regulated oncogenes and down-regulated tumor suppressors upon CR

Gene Symbol	FC	Adjusted P-value	Cancer relevance
Pck1	4.39	1.62E-04	1, 2
Aldh1a1	2.45	1.76E-04	3
Rrm2	4.02	2.05E-04	4
Cemip	4.25	2.27E-04	5
Tns4	2.27	1.28E-03	6, 7, 8
Abca1	3.90	1.66E-03	9
Gsta3	3.00	2.04E-03	10, 11
Rab30	2.32	1.22E-02	12, 13
Sgk1	1.86	3.90E-02	14
Rnasel	-1.74	2.37E-03	15, 16, 17, 18, 19, 20, 21, 22
Irf1	-1.54	2.43E-03	23, 24, 25, 26, 27
Arntl	-1.87	1.56E-02	28, 29, 30, 31

1. Grasmann G, Smolle E, Olschewski H, Leithner K. Gluconeogenesis in cancer cells - Repurposing of a starvation-induced metabolic pathway? Biochim Biophys Acta Rev Cancer 1872, 24-36 (2019).
2. Xiang J, et al. Transcriptomic changes associated with PCK1 overexpression in hepatocellular carcinoma cells detected by RNA-seq. Genes & Diseases, (2019).
3. Tomita H, Tanaka K, Tanaka T, Hara A. Aldehyde dehydrogenase 1A1 in stem cells and cancer. Oncotarget 7, 11018-11032 (2016).
4. Liu X, et al. Ribonucleotide reductase small subunit M2 serves as a prognostic biomarker and predicts poor survival of colorectal cancers. Clin Sci (Lond) 124, 567-578 (2013).
5. Fink SP, et al. Induction of KIAA1199/CEMIP is associated with colon cancer phenotype and poor patient survival. Oncotarget 6, 30500-30515 (2015).
6. Tang X, et al. A mechanically-induced colon cancer cell population shows increased metastatic potential. Mol Cancer 13, 131 (2014).
7. Kim S, Kim N, Kang K, Kim W, Won J, Cho J. Whole Transcriptome Analysis Identifies TNS4 as a Key Effector of Cetuximab and a Regulator of the Oncogenic Activity of KRAS Mutant Colorectal Cancer Cell Lines. Cells 8, (2019).
8. Sawazaki S, et al. Clinical Significance of Tensin 4 Gene Expression in Patients with Gastric Cancer. In Vivo 31, 1065-1071 (2017).
9. Aguirre-Portoles C, Feliu J, Reglero G, Ramirez de Molina A. ABCA1 overexpression worsens colorectal cancer prognosis by facilitating tumour growth and caveolin-1-dependent invasiveness, and these effects can be ameliorated using the BET inhibitor apabetalone. Mol Oncol 12, 1735-1752 (2018).
10. Xiao Y, Meierhofer D. Glutathione Metabolism in Renal Cell Carcinoma Progression and Implications for Therapies. Int J Mol Sci 20, (2019).
11. Al Ahmad A, et al. Papillary Renal Cell Carcinomas Rewire Glutathione Metabolism and Are Deficient in Both Anabolic Glucose Synthesis and Oxidative Phosphorylation. Cancers (Basel) 11, (2019).
12. Regnier M, et al. Insights into the role of hepatocyte PPARalpha activity in response to fasting. Mol Cell Endocrinol 471, 75-88 (2018).
13. Vidyasekar P, et al. Genome Wide Expression Profiling of Cancer Cell Lines Cultured in Microgravity Reveals Significant Dysregulation of Cell Cycle and MicroRNA Gene Networks. PLoS One 10, e0135958 (2015).
14. Lang F, Perrotti N, Stournaras C. Colorectal carcinoma cells--regulation of survival and growth by SGK1. Int J Biochem Cell Biol 42, 1571-1575 (2010).
15. Long TM, et al. RNase-L deficiency exacerbates experimental colitis and colitis-associated cancer. Inflamm Bowel Dis 19, 1295-1305 (2013).
16. Burke JM, Lester ET, Tauber D, Parker R. RNase L promotes the formation of unique ribonucleoprotein granules distinct from stress granules. J Biol Chem 295, 1426-1438 (2020).
17. Burke JM, Moon SL, Matheny T, Parker R. RNase L Reprograms Translation by Widespread mRNA Turnover Escaped by Antiviral mRNAs. Mol Cell 75, 1203-1217 e1205 (2019).
18. Kruger S, et al. The additive effect of p53 Arg72Pro and RNASEL Arg462Gln genotypes on age of disease onset in Lynch syndrome patients with pathogenic germline mutations in MSH2 or MLH1. Cancer Lett 252, 55-64 (2007).
19. Kruger S, et al. Arg462Gln sequence variation in the prostate-cancer-susceptibility gene RNASEL and age of onset of hereditary non-polyposis colorectal cancer: a case-control study. Lancet Oncol 6, 566-572 (2005).
20. Batman G, Oliver AW, Zehbe I, Richard C, Hampson L, Hampson IN. Lopinavir up-regulates expression of the antiviral protein ribonuclease L in human papillomavirus-positive cervical carcinoma cells. Antivir Ther 16, 515-525 (2011).
21. Banerjee S, et al. OAS-RNase L innate immune pathway mediates the cytotoxicity of a DNA-demethylating drug. Proc Natl Acad Sci U S A 116, 5071-5076 (2019).
22. Banerjee S, et al. RNase L is a negative regulator of cell migration. Oncotarget 6, 44360-44372 (2015).
23. Zenke K, Muroi M, Tanamoto KI. IRF1 supports DNA binding of STAT1 by promoting its phosphorylation. Immunol Cell Biol 96, 1095-1103 (2018).
24. Hong M, et al. IRF1 inhibits the proliferation and metastasis of colorectal cancer by suppressing the RAS-RAC1 pathway. Cancer Manag Res 11, 369-378 (2019).
25. Komatsu Y, Christian SL, Ho N, Pongnopparat T, Licursi M, Hirasawa K. Oncogenic Ras inhibits IRF1 to promote viral oncolysis. Oncogene 34, 3985-3993 (2015).
26. Ohsugi T, et al. Anti-apoptotic effect by the suppression of IRF1 as a downstream of Wnt/beta-catenin signaling in colorectal cancer cells. Oncogene 38, 6051-6064 (2019).
27. Shao L, et al. IRF1 Inhibits Antitumor Immunity through the Upregulation of PD-L1 in the Tumor Cell. Cancer Immunol Res 7, 1258-1266 (2019).
28. Gwon DH, et al. BMAL1 Suppresses Proliferation, Migration, and Invasion of U87MG Cells by Downregulating Cyclin B1, Phospho-AKT, and Metalloproteinase-9. Int J Mol Sci 21, (2020).
29. Tang Q, et al. Circadian Clock Gene Bmal1 Inhibits Tumorigenesis and Increases Paclitaxel Sensitivity in Tongue Squamous Cell Carcinoma. Cancer Res 77, 532-544 (2017).
30. Fekry B, et al. Incompatibility of the circadian protein BMAL1 and HNF4alpha in hepatocellular carcinoma. Nat Commun 9, 4349 (2018).
31. Yeh CM, et al. Epigenetic silencing of ARNTL, a circadian gene and potential tumor suppressor in ovarian cancer. Int J Oncol 45, 2101-2107 (2014).

Supplementary Table 7. Experimental validation targets

Ensembl ID	Gene Symbol	Gene Description	Categorization	Potential Therapeutic Target	FC	adj. P-value
ENSMUSG00000020826	*Nos2*	nitric oxide synthase 2, inducible	cancer-associated/Sirtuin Signaling Pathway	yes	-2.92	1.39E-02
ENSMUSG00000039005	*Tlr4*	toll-like receptor 4	cancer-associated	yes	-1.77	1.23E-03
ENSMUSG00000034855	*Cxcl10*	chemokine (C-X-C motif) ligand 10	cancer-associated	yes	-2.03	3.80E-03
ENSMUSG00000036986	*Pml*	promyelocytic leukemia	telomeric		-1.43	3.57E-02
ENSMUSG00000029167	*Ppargc1a*	peroxisome proliferative activated receptor, gamma, coactivator 1 alpha	metabolism/cancer-associated/Sirtuin Signaling Pathway		-1.65	1.22E-02
ENSMUSG00000027513	*Pck1*	phosphoenolpyruvate carboxykinase 1, cytosolic	Sirtuin Signaling Pathway		4.39	1.62E-04
ENSMUSG00000015243	*Abca1*	ATP-binding cassette, sub-family A (ABC1), member 1	Sirtuin Signaling Pathway/cancer cell metabolism		3.90	1.66E-03
ENSMUSG00000025934	*Gsta3*	glutathione S-transferase, alpha 3	glutathione metabolism		3.00	2.04E-03
ENSMUSG00000020649	*Rrm2*	ribonucleotide reductase M2	cancer-associated, cell cycle, glutathione metabolism	yes	4.02	2..05E-04
ENSMUSG00000026479	*Lamc2*	laminin, gamma 2	cancer-associated		1.75	6.78E-03
ENSMUSG00000021822	*Plau*	plasminogen activator, urokinase	cancer-associated		1.78	1.48E-03

Indicates top genes for future qPCR validation.

Supplementary Table 8. IPA generated enriched canonical pathways

(A) 467 Unique Duodenal CR DEGs ($p < 10^{-4}$)

Ingenuity Canonical Pathways	Molecules[a]	p-value
LPS/IL-1 Mediated Inhibition of RXR Function	20	4.17E-08
Xenobiotic Metabolism Signaling	23	6.76E-08
PXR/RXR Activation	11	7.59E-08
Glutathione-mediated Detoxification	6	1.20E-05
Superpathway of Melatonin Degradation	8	1.74E-05
Estrogen Biosynthesis	7	2.14E-05
Antigen Presentation Pathway	6	3.24E-05
Nicotine Degradation III	7	3.63E-05
Triacylglycerol Degradation	7	5.13E-05
Interferon Signaling	6	6.03E-05
Aryl Hydrocarbon Receptor Signaling	12	6.31E-05
Melatonin Degradation I	7	6.92E-05
Acyl-CoA Hydrolysis	4	8.71E-05

[a]Number of 467 Unique Duodenal DEGs in Category

(B) Cancer-associated Genes ($p < 10^{-4}$)

Ingenuity Canonical Pathways	Molecules[a]	p-value
LPS/IL-1 Mediated Inhibition of RXR Function	10	6.92E-07
Sirtuin Signaling Pathway	11	1.32E-06
PXR/RXR Activation	6	2.00E-06
Xenobiotic Metabolism Signaling	10	5.37E-06
Sphingomyelin Metabolism	3	1.55E-05
LXR/RXR Activation	6	8.13E-05

[a]Number of Cancer-associated Genes in Category

(C) Telomere Genes ($p < 0.01$)

Ingenuity Canonical Pathways	Molecules[a]	p-value
Sirtuin Signaling Pathway	5	9.77E-05
UDP-D-xylose and UDP-D-glucuronate Biosynthesis	1	3.63E-03
RAR Activation	3	4.37E-03
PXR/RXR Activation	2	4.79E-03
Cell Cycle: G1/S Checkpoint Regulation	2	6.03E-03
Cyclins and Cell Cycle Regulation	2	8.71E-03

[a]Number of Telomere Genes in Category

(D) Epithelial Cell Genes ($p < 10^{-4}$)

Ingenuity Canonical Pathways	Molecules[a]	p-value
Superpathway of Melatonin Degradation	8	1.95E-09
Nicotine Degradation III	7	1.12E-08
LPS/IL-1 Mediated Inhibition of RXR Function	12	2.69E-08
Melatonin Degradation I	7	2.88E-08
Nicotine Degradation II	7	3.39E-08
Estrogen Biosynthesis	6	2.45E-07
Bupropion Degradation	5	4.57E-07
Xenobiotic Metabolism Signaling	12	7.24E-07
Acetone Degradation I (to Methylglyoxal)	5	1.41E-06
PXR/RXR Activation	6	4.79E-06
Glutathione-mediated Detoxification	4	1.78E-05
Glucose and Glucose-1-phosphate Degradation	3	5.13E-05

[a]Number of Epithelial Cell Genes in Category

(E) Immune System Genes ($p < 10^{-4}$)

Ingenuity Canonical Pathways	Molecules[a]	p-value
Antigen Presentation Pathway	6	1.45E-07
Interferon Signaling	6	2.82E-07
Type I Diabetes Mellitus Signaling	8	3.24E-06
Communication between Innate and Adaptive Immune Cells	6	2.29E-05
T Helper Cell Differentiation	6	2.51E-05
Retinoic acid Mediated Apoptosis Signaling	5	3.63E-05
Crosstalk between Dendritic Cells and Natural Killer Cells	6	3.89E-05
iCOS-iCOSL Signaling in T Helper Cells	7	3.98E-05
Th1 Pathway	7	4.57E-05
iNOS Signaling	5	5.25E-05

[a]Number of Immune System Genes in Category

Supplementary Table 9. IPA canonical pathway: Sirtuin Signaling Pathway

(A)

Category	Molecules[a]	p-value
Cancer-associated	11	1.32E-06
Telomeres	5	9.77E-05
Epithelial	8	8.51E-04
467 Unique	15	1.38E-03

[a]Number of Genes in Category

(B)

Ensemble ID	Gene Symbol	Gene Description	FC	adj. P-value
ENSMUSG00000027513	*Pck1*	phosphoenolpyruvate carboxykinase 1, cytosolic	4.39	1.62E-04
ENSMUSG00000003849	*Nqo1*	NAD(P)H dehydrogenase, quinone 1	2.26	7.34E-04
ENSMUSG00000026773	*Pfkfb3*	6-phosphofructo-2-kinase/fructose-2,6-biphosphatase 3	-2.19	1.01E-03
ENSMUSG00000022383	*Ppara*	peroxisome proliferator activated receptor alpha	2.49	1.34E-03
ENSMUSG00000005125	*Ndrg1*	N-myc downstream regulated gene 1	2.65	1.48E-03
ENSMUSG00000015243	*Abca1*	ATP-binding cassette, sub-family A (ABC1), member 1	3.90	1.66E-03
ENSMUSG00000042688	*Mapk6*	mitogen-activated protein kinase 6	1.51	1.98E-03
ENSMUSG00000031583	*Wrn*	Werner syndrome homolog (human)	-1.59	2.36E-03
ENSMUSG00000020538	*Srebf1*	sterol regulatory element binding transcription factor 1	1.57	3.30E-03
ENSMUSG00000039231	*Suv39h1*	suppressor of variegation 3-9 homolog 1 (Drosophila)	1.65	5.63E-03
ENSMUSG00000029167	*Ppargc1a*	peroxisome proliferative activated receptor, gamma, coactivator 1 alpha	-1.65	1.22E-02
ENSMUSG00000020826	*Nos2*	nitric oxide synthase 2, inducible	-2.92	1.39E-02
ENSMUSG00000055116	*Arntl*	aryl hydrocarbon receptor nuclear translocator-like	-1.87	1.56E-02
ENSMUSG00000041238	*Rbbp8*	retinoblastoma binding protein 8	1.70	2.25E-02
ENSMUSG00000026187	*Xrcc5*	X-ray repair complementing defective repair in Chinese hamster cells 5	1.58	3.01E-02

(A) Number of common genes in the enriched canonical pathway, the Sirtuin Signaling Pathway, per gene category subset. **(B)** 15 significant genes in the enriched ingenuity canonical pathway, the Sirtuin Signaling Pathway, for the duodenum mucosa samples of caloric restriction vs. *ad libitum* control mice (adj. p-value < 0.05 at |FC|>1.5). Fischer's exact test is used to calculate p-values in IPA. Sirtuin 3 was also downregulated in the telomere subset, but had FC = -1.38 and thus not counted in the 467 Unique DEGs.

Supplementary Table 10. Comparison of 18 microarray DEGs in duodenum mucosa with CR response defined by RT-PCR in GI tract tissues.

(A) Comparison of 18 m-array DEGs (FC values in Duodenum mucosa) with the response pattern of the same genes detected in RT-PCR in GI tract tissues. RT-PCR gene expression is categorized by the following: -1: down-regulated DEG; 0: not significant changes; 1: upregulated DEG. Parts of GI tract: D: Duodenum, J: Jejunum, I: Ileum, PC: Proximal Colon, DC: Distant Colon, S: Stomach. See details in Methods. **(B)** Kendall Tau Correlation coefficients of the m-array DEGs in DM and RT-PCR patterns (-1, 0, 1) among different parts of GI tract.

(A)

Gene Symbol	Microarray DEGs: Fold change (FC)	GI tract. RT-PCR data. 1: up-reg., 0: no change, -1: down-reg.							Cancer-associated and immune system annotations of micro-array data (Suppl. Data 1)	
	D	D	J	I	PC	DC	S	PCA 1 Score*	cancer-associated	immune system
Acox2	3.37	1	1	0	1	1	0	0.78		
Gsta3	3.00	1	1	1	1	1	1	1.27	1	
Vldlr	2.81	1	0	0	1	0	0	0.24	1	
Scd1	2.72	1	1	1	1	1	0	1.01	1	1
Ppara	2.49	1	0	1	0	0	-1	-0.10	1	
Mgst1	2.37	1	1	1	1	1	0	1.01	1	1
Acot4	2.34	1	0	0	1	0	0	0.24		
Mgst2	1.96	1	1	1	1	0	1	0.99	1	
Mt2	1.94	1	1	1	1	1	1	1.27	1	
Cd36	1.86	1	0	0	0	0	1	0.17	1	1
Gsta4	1.48	1	0	0	1	0	0	0.24		
Myd88	-1.41	0	-1	0	0	0	0	-0.59		
Tlr3	-1.41	-1	-1	-1	0	0	0	-1.07		
Irf1	-1.54	-1	-1	0	0	-1	-1	-1.37	-1	-1
Reg3b	-1.60	0	0	-1	1	1	0	0.03	-1	-1
Stat1	-1.66	-1	-1	-1	-1	-1	-1	-1.92	-1	-1
Reg3g	-1.70	0	-1	0	0	0	0	-0.59	-1	
Oas1a	-1.74	-1	-1	-1	0	-1	-1	-1.60		-1

(B)

Kendall's Correlations	CR_DM_FC (microarray)	D	S	J	I	PC	DC	Average Corr.**
CR_DM_FC (microarray)	1	0.68	0.31	0.65	0.55	0.53	0.51	0.54
D	0.68	1	0.55	0.78	0.70	0.68	0.55	0.54
S	0.31	0.55	1	0.56	0.42	0.50	0.53	0.48
J	0.65	0.78	0.56	1	0.69	0.76	0.75	0.70
I	0.55	0.70	0.42	0.69	1	0.45	0.48	0.55
PC	0.53	0.68	0.50	0.76	0.45	1	0.70	0.60
DC	0.51	0.55	0.53	0.75	0.48	0.70	1	0.59

*Principal component 1 (PC1) score values; Spearman corr. between the microarray DM DEG fold change (FC) and qPCR PC1 score values of the 18 genes: $r=0.77$, $p<0.001$. Freidman ANOVA (Similarity test: $p=0.22$)

** (Sum of correlation coefficients)/(n-1); n=7 at $p<0.05$.

Supplementary Table 11. CR DEGs immune cell-type classification

(A) human T cells

Gene Symbol	Immune Cell Type	FC	adj. P-value
Cth	Human T Regulatory Cells	1.62	7.85E-03
H2-Ea-ps	Human T Regulatory Cells	-2.08	2.32E-02
Mfsd7c	Human T Regulatory Cells	5.57	2.00E-04
Npdc1	Human All T cells	-1.55	2.98E-03
Sesn1	Human T Regulatory Cells	-1.58	6.33E-03
Slc6a6	Human T Regulatory Cells	1.55	1.29E-02
Zbtb16	Human CD8+T Cells	2.63	3.63E-03

(B) murine macrophages

Gene Symbol	Immune Cell Type	FC	adj. P-value
Cxcl10	Murine M1 Macrophages	-2.03	3.80E-03
Ddx60	Murine M1 Macrophages	-2.13	1.49E-02
Gbp6	Murine M1 Macrophages	-2.15	1.81E-04
H2-Q6	Murine M1 Macrophages	-1.56	1.33E-02
Herc6	Murine M1 Macrophages	-3.23	1.01E-03
Ifi44	Murine M1 Macrophages	-4.94	3.04E-04
Ifit1	Murine M1 Macrophages	-3.36	2.57E-03
Ifit2	Murine M1 Macrophages	-2.30	6.83E-03
Ms4a4c	Murine M1 Macrophages	-1.53	4.01E-02
Mx2	Murine M1 Macrophages	-1.62	1.64E-02
Pecr	Murine Macrophages	1.97	1.48E-02
Stat1	Murine M1 Macrophages	-1.66	2.37E-03
Stat2	Murine M1 Macrophages	-1.51	3.36E-03
Tlr4	Murine Macrophages	-1.77	1.23E-03
Xaf1	Murine M1 Macrophages	-1.71	1.22E-02

(C) human monocytes

Gene Symbol	Immune Cell Type	FC	adj. P-value
Aldh1a1	Human Classical Monocytes	2.45	1.76E-04
Aldh1a7	Human Classical Monocytes	2.63	4.24E-04
Fbp1	Human Intermediate Monocytes	1.67	4.50E-03
Gbp6	Human Intermediate Monocytes	-2.15	1.81E-04
Mgst1	Human Classical Monocytes	2.37	3.45E-04
Mosc1/Marc1	Human Classical Monocytes	3.07	1.06E-03
Nkg7	Human Intermediate Monocytes	-1.63	2.21E-03
Rdh16	Human Intermediate Monocytes	-1.54	6.18E-03
Rdh9	Human Intermediate Monocytes	1.60	7.16E-03
Scd1	Human Intermediate Monocytes	2.72	9.51E-03
Setbp1	Human Nonclassical Monocytes	-2.14	1.10E-03
Tgm2	Human Intermediate Monocytes	-3.10	4.48E-03

(D) human dendritic cells

Gene Symbol	Immune Cell Type	FC	adj. P-value
Cd36	Human Monocyte Derived DC's	1.86	2.21E-03
Cxcl10	Human Mature DC's	-2.03	3.80E-03
Fcer2a	Human Monocyte Derived DC's	-1.90	7.30E-03
Gbp6	Human Mature DC's	-2.15	1.81E-04
Ifit1	Human Mature DC's	-3.36	2.57E-03
Ifit3	Human Mature DC's	-2.22	2.26E-02
Mx2	Human Mature DC's	-1.62	1.64E-02
Oasl2	Human Mature DC's	-2.37	6.78E-03
Tnfsf10	Human Mature DC's	-2.06	1.48E-03
Usp18	Human Mature DC's	-2.55	6.24E-03

(E) human neutrophils

Gene Symbol	Immune Cell Type	FC	adj. P-value
Sema3c	Human Mature Neutrophils	1.51	1.03E-02

(F) 8 genes with multiple cell specific classifications

Gene Symbol	Immune Cell Types
Nkg7	Human B-cell and Human Intermediate Monocyte
Setbp1	Human B-cell and Human Nonclassicial Monocyte
Cxcl10	Murine M1 Macrophage and Human Mature DC
Gbp6	Murine M1 Macrophage, Human Intermediate Monocyte, and Human Mature DC
Ifit1	Murine M1 Macrophage and Human Mature DC
Ifit3	Human B-cell and Human Mature DC
Mx2	Murine M1 Macrophage and Human Mature DC
H2-Ea-ps	Human T Regulatory and Human B-cell

(G) human B cells

Gene Symbol	Immune Cell Type	FC	adj. P-value
Abca1	Human B-cells	3.90	1.66E-03
Bank1	Human B-cells	-1.89	4.98E-02
Bcl11a	Human B-cells	-1.54	3.74E-02
Cd72	Human B-cells	-1.80	5.71E-03
Ciita	Human B-cells	-1.55	2.59E-02
Cr1l	Human B-cells	-1.51	1.35E-02
Ephx1	Human B-cells	2.24	3.59E-04
Etv3	Human B-cells	-1.52	8.55E-03
H2-Dma	Human B-cells	-1.62	8.87E-04
H2-Ea-ps	Human B-cells	-2.08	2.32E-02
Ifi27l2a	Human B-cells	-1.54	1.93E-03
Ifit3	Human B-cells	-2.22	2.26E-02
Ly86	Human B-cells	-2.04	5.78E-03
Nkg7	Human B-cells	-1.63	2.21E-03
Parp14	Human B-cells	-1.84	3.93E-03
Rab30	Human B-cells	2.32	1.22E-02
Setbp1	Human B-cells	-2.14	1.10E-03
Sp140	Human B-cells	-1.88	7.34E-04
Spib	Human B-cells	-1.62	2.90E-02

Enriched genes in immune cells (>2-fold difference) for human and mouse expression profiles when immune cell types were compared (Lyons et al., 2017). Human genes were converted to mouse orthologs using MGI Batch Query.

(H) ImmPort gene list classification of immune response CR DEGs

Immune System Classification	Human Gene Symbol	Mouse Gene Symbol	Gene Description	CR mouse FC	adj. P-value
TNF Family Members	*TNFSF10*	*Tnfsf10*	tumor necrosis factor (ligand) superfamily, member 10	-2.06	1.48E-03
	TNFSF13B	*Tnfsf13b*	tumor necrosis factor (ligand) superfamily, member 13b	-1.67	3.76E-02
TNF Family Members Receptors	*TNFRSF11A*	*Tnfrsf11a*	tumor necrosis factor receptor superfamily, member 11a	-1.70	3.76E-02
	TNFRSF21	*Tnfrsf21*	tumor necrosis factor receptor superfamily, member 21	1.67	2.03E-02
Chemokines	*CCL28*	*Ccl28*	chemokine (C-C motif) ligand 28	-1.66	9.07E-03
	CXCL10	*Cxcl10*	chemokine (C-X-C motif) ligand 10	-2.03	3.80E-03
	CXCL9	*Cxcl9*	chemokine (C-X-C motif) ligand 9	-1.79	4.96E-03
	CKLF	*Klf5*	Kruppel-like factor 15	1.60	4.22E-04
	SEMA3C	*Sema3c*	sema domain, immunoglobulin domain (Ig), short basic domain, secreted, (semaphorin) 3C	1.51	1.03E-02
	SEMA6D	*Sema6d*	sema domain, transmembrane domain (TM), and cytoplasmic domain, (semaphorin) 6D	-1.54	1.60E-02
Cytokine Receptors	*ANGPTL4*	*Angptl4*	angiopoietin-like 4	2.69	3.14E-03
	NOR1	*Plscr1*	phospholipid scramblase	2.81	1.54E-04
	MTNR1B, MT2	*Mt2*	metallothionein 2	1.94	3.12E-03
	PPARA	*Ppara*	peroxisome proliferator activated receptor alpha	2.49	1.34E-03
	PRLR	*Prlr*	prolactin receptor	-1.51	3.58E-02
Interleukin Receptors	*IL2RG*	*Il2rg*	interleukin 2 receptor, gamma chain	-2.18	1.62E-04
TGF-b Family Member Receptors	*TGFBR2*	*Tgfbr2*	transforming growth factor, beta receptor II	1.64	1.12E-02
NK Cells	*FCER1G*	*Fcer1g*	Fc receptor, IgE, high affinity I, gamma polypeptide	-1.63	5.74E-03
	HLA-A	*H2-Q6*	histocompatibility 2, Q region locus 6	-1.56	1.33E-02
	NGK7	*Nkg7*	natural killer cell group 7 sequence	-1.63	2.21E-03
Antigen Presenting Cells	*CLEC4M*	*Cd209a*	CD209a antigen	-1.56	1.48E-02
	CIITA	*Ciita*	class II transactivator	-1.55	2.59E-02
	HLA-DMA	*H2-DMa*	histocompatibility 2, class II, locus DMa	-1.62	8.87E-04
	TAP1	*Tap1*	transporter 1, ATP-binding cassette, sub-family B (MDR/TAP)	-1.51	1.86E-02

The gene lists available at https://www.immport.org/shared/genelists were converted to mouse orthologs using MGI Batch Query.

Supplementary Table 12. Gene symbols associated with multiple probe sets

Ensemble ID	Gene Symbol	# of probe sets	Gene Accession	Gene Description	FC	adj. P-value
ENSMUSG00000052392	*Acot4*	2	NM_134247	acyl-CoA thioesterase 4	2.34	2.87E-03
ENSMUSG00000027597	*Ahcy*	3	NM_016661	S-adenosylhomocysteine hydrolase	1.76	1.17E-02
ENSMUSG00000028028	*Alpk1*	3	NM_027808	alpha-kinase 1	-2.64	4.88E-04
ENSMUSG00000071324	*Armc2 *isoform B*	2	NM_001034858	armadillo repeat containing 2	-1.88	8.52E-04
ENSMUSG00000071324	*Armc2 *isoform A*			armadillo repeat containing 2	1.65	5.01E-03
ENSMUSG00000078566	*Bnip3*	2	NM_009760	BCL2/adenovirus E1B interacting protein 3	2.20	8.95E-03
ENSMUSG00000059005	*Hnrnpa3*	9	NM_053263, NM_146130, ENSMUST00000111964	heterogeneous nuclear ribonucleoprotein A3	1.69	2.21E-03
ENSMUSG00000028184	*Lphn2*	5	NM_001081298	latrophilin 2	-1.64	2.29E-03
ENSMUSG00000032418	*Me1*	2	NM_008615	malic enzyme 1, NADP(+)-dependent, cytosolic	1.92	7.02E-04
ENSMUSG00000066595	*Mfsd7b*	3	BC010797, NM_001081259	major facilitator superfamily domain containing 7B	1.84	2.43E-03
ENSMUSG00000032959	*Pebp1*	2	ENSMUST00000036951, NM_018858	phosphatidylethanolamine binding protein 1	1.62	1.03E-02
ENSMUSG00000032369	*Plscr1*	2	NM_011636	phospholipid scramblase 1	2.81	1.54E-04
ENSMUSG00000029167	*Ppargc1a*	2	NM_008904, NR_027710	peroxisome proliferative activated receptor, gamma, coactivator 1 alpha	-1.65	1.22E-02
ENSMUSG00000070327	*Rnf213*	9	AK173199, ENSMUST00000131035	ring finger protein 213	-2.19	3.88E-03
ENSMUSG00000027227	*Sord*	2	NM_146126	sorbitol dehydrogenase	1.56	9.32E-03
ENSMUSG00000070034	*Sp110*	4	NM_175397	Sp110 nuclear body protein	-1.88	1.62E-04
ENSMUSG00000037926	*Ssh2*	2	NM_177710	slingshot homolog 2 (Drosophila)	-1.54	9.45E-03

Annotation of Armc2 isoforms:

Armc2 *isoform A	pos. regulated	GPL6246, 10368881 (ID_REF), NM_001034858, chr10:42008653-42008725 (SPOT ID), 2nd exon longest isoform
Armc2 *isoform B	neg. regulated	GPL6246, 10368859 (ID_REF), NM_001034858, XM_006512653, BC172168, chr10:41914993-42007709, (SPOT ID), longest isoform

One gene, *Armc2*, had both upregulation and downregulation data, leading to the distinction of isoform A (upregulated) and isoform B (downregulated). The probe set with the lowest adj. p-value was chosen when a specific gene symbol had all upregulated or downregulated expression data for all associated probe sets.